



<b>Publication Year</b>	2018
<b>Acceptance in OA</b>	2020-12-28T15:52:24Z
<b>Title</b>	Formation of a Malin 1 analogue in IllustrisTNG by stimulated accretion
<b>Authors</b>	Zhu, Qirong, Xu, Dandan, GASPARI, MASSIMO, Rodriguez-Gomez, Vicente, Nelson, Dylan, Vogelsberger, Mark, Torrey, Paul, Pillepich, Annalisa, Zjupa, Jolanta, Weinberger, Rainer, MARINACCI, FEDERICO, Pakmor, Rüdiger, Genel, Shy, Li, Yuexing, Springel, Volker, Hernquist, Lars
<b>Publisher's version (DOI)</b>	10.1093/mnrasl/sly111
<b>Handle</b>	<a href="http://hdl.handle.net/20.500.12386/29231">http://hdl.handle.net/20.500.12386/29231</a>
<b>Journal</b>	MONTHLY NOTICES OF THE ROYAL ASTRONOMICAL SOCIETY
<b>Volume</b>	480

# Formation of a Malin 1 analogue in IllustrisTNG by stimulated accretion

Qirong Zhu,<sup>1,2★</sup> Dandan Xu,<sup>3</sup> Massimo Gaspari,<sup>4†</sup> Vicente Rodriguez-Gomez,<sup>5</sup>  
Dylan Nelson,<sup>6</sup> Mark Vogelsberger,<sup>7‡</sup> Paul Torrey,<sup>7§</sup> Annalisa Pillepich,<sup>8</sup>  
Jolanta Zjupa,<sup>3,9</sup> Rainer Weinberger,<sup>3</sup> Federico Marinacci,<sup>7</sup> Rüdiger Pakmor,<sup>3</sup>  
Shy Genel,<sup>10,11</sup> Yuexing Li,<sup>1</sup> Volker Springel<sup>3,6,12</sup> and Lars Hernquist<sup>2</sup>

<sup>1</sup>Department of Astronomy & Astrophysics, Institute for Cosmology and Gravity, The Pennsylvania State University, PA 16802, USA

<sup>2</sup>Harvard-Smithsonian Center for Astrophysics, Harvard University, 60 Garden Street, Cambridge, MA 02138, USA

<sup>3</sup>Heidelberger Institut für Theoretische Studien, Schloss-Wolfsbrunnengasse 35, D-69118 Heidelberg, Germany

<sup>4</sup>Department of Astrophysical Sciences, Princeton University, 4 Ivy Lane, Princeton, NJ 08544-1001, USA

<sup>5</sup>Department of Physics & Astronomy, Johns Hopkins University, 3400 N. Charles Street, Baltimore, MD 21218, USA

<sup>6</sup>Max-Planck-Institut für Astrophysik, Karl-Schwarzschild-Str. 1, D-85748 Garching, Germany

<sup>7</sup>Department of Physics, Kavli Institute for Astrophysics and Space Research, MIT, Cambridge, MA 02139, USA

<sup>8</sup>Max-Planck-Institut für Astronomie, Königstuhl 17, D-69117 Heidelberg, Germany

<sup>9</sup>Institut für Theoretische Physik, Philosophenweg 16, D-69120 Heidelberg, Germany

<sup>10</sup>Center for Computational Astrophysics, Flatiron Institute, 162 Fifth Avenue, New York, NY 10010, USA

<sup>11</sup>Columbia Astrophysics Laboratory, Columbia University, 550 West 120th Street, New York, NY 10027, USA

<sup>12</sup>Zentrum für Astronomie der Universität Heidelberg, ARI, Mönchhofstrasse 12-14, D-69120 Heidelberg, Germany

Accepted 2018 June 10. Received 2018 May 21; in original form 2018 March 29

## ABSTRACT

The galaxy Malin 1 contains the largest stellar disc known but the formation mechanism of this structure has been elusive. In this paper, we report a Malin 1 analogue in the 100 Mpc IllustrisTNG simulation and describe its formation history. At redshift zero, this massive galaxy, having a maximum circular velocity  $V_{\max}$  of  $430 \text{ km s}^{-1}$ , contains a 100 kpc gas/stellar disc with morphology similar to Malin 1. The simulated galaxy reproduces well many observed features of Malin 1's vast disc, including its stellar ages, metallicities, and gas rotation curve. We trace the extended disc back in time and find that a large fraction of the cold gas at redshift zero originated from the cooling of hot halo gas, triggered by the merger of a pair of intruding galaxies. Our finding provides a novel way to form large galaxy discs as extreme as Malin 1 within the current galaxy formation framework.

**Key words:** methods: numerical – galaxies: evolution – galaxies: formation – galaxies: individual: Malin 1.

## 1 INTRODUCTION

Malin 1, discovered by Bothun et al. (1987), has one of the largest stellar discs known. With a diameter of at least 200 kpc, its angular size on the sky is wider than one arcmin even though Malin 1 is a quite distant object ( $z \sim 0.09$ ). Malin 1 is a prime example of giant low surface brightness (GLSB) galaxies, characterized by their extended low surface brightness disc and high gas content (Sprayberry et al. 1995). Other examples of extreme GLSB galaxies exist (e.g. UGC1382, Hagen et al. 2016) with properties similar to Malin 1. Without the extended outer discs, Malin 1 and UGC1382

would otherwise appear similar to normal massive galaxies (Barth 2007; Hagen et al. 2016).

Observations of the Malin 1 disc are still limited due to its low surface brightness. Recent observations by Boissier et al. (2016) show spectacular spiral structure made of relatively young ( $\sim 0.1\text{--}3$  Gyr) stars with metallicities between 0.1 and  $1Z_{\odot}$  with no apparent stellar age gradient across the disc. A more surprising feature is the large mass with  $V_{\max}$  above  $400 \text{ km s}^{-1}$  if the (poorly constrained) inclination is low (consistent with, e.g. Galaz et al. 2015).

It remains a great challenge to understand the physical process behind a disc that is at least five times larger than the Milky Way. This single object, being an extreme outlier, is a severe test for the current theory of galaxy formation and modified gravity (Lelli Fraternali & Sancisi 2010; Boissier et al. 2016). In this Letter, we report a Malin 1 analogue from the IllustrisTNG simulations. At  $z = 0$ , this galaxy has an extended gas/stellar disc with size/morphology

\* E-mail: zhuqirong1874@gmail.com

† Einstein and Spitzer Fellow.

‡ Alfred P. Sloan Fellow.

§ Hubble Fellow.

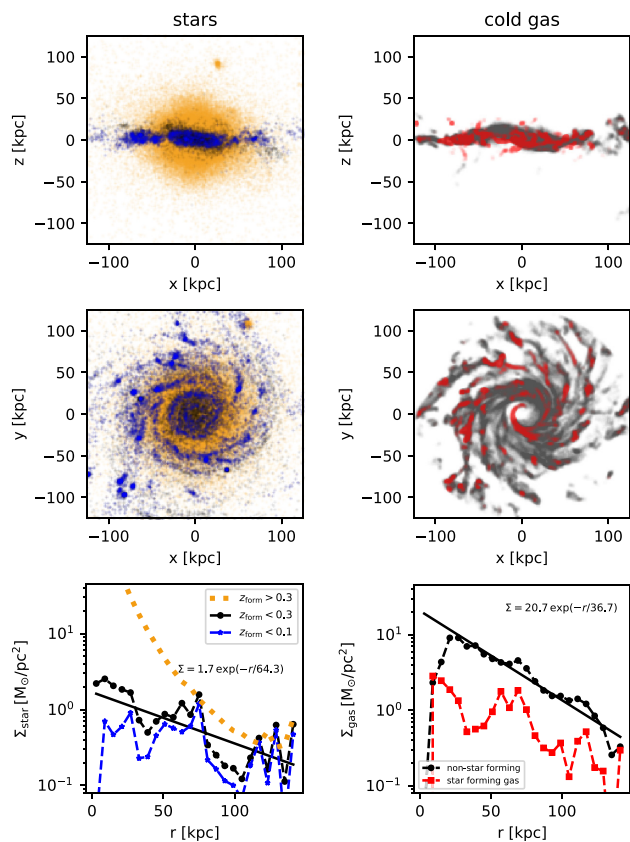


**Figure 1.** Edge-on (top row) and face-on (middle row) views of the stellar (left) and gas (right) disc. Newly formed stars are shown in blue ( $z_{\text{form}} < 0.1$ ) and grey ( $z_{\text{form}} < 0.3$ ) while old stars in orange. The stellar surface density with  $z_{\text{form}} < 0.3$  follows an exponential profile with a scale length of 64 kpc. Outside of 100 kpc, the newly formed stellar disc is comparable to the existing stellar mass (the dotted line) while the luminosity will be dominated by the young population. In the right-hand column, we show the cold gas in grey and star forming-gas in red. The surface density profile of the cold gas follows an exponential profile with a scale length of 37 kpc.

similar to Malin 1. We then trace the extended disc back in time and find that a large fraction of the neutral gas came from the cooling of hot halo gas, triggered by a merger event involving a pair of intruding galaxies, a process we term ‘stimulated accretion’. In what follows, we first describe our methods and present our main results in Section 2. We discuss our findings and present observational tests in Section 3 and conclude in Section 4.

## 2 METHODS AND RESULTS

We identified this galaxy during our search for GLSB galaxies (Zhu et. al, in preparation) in the IllustrisTNG simulation suite (Marinacci et al. 2017b; Naiman et al. 2018; Nelson et al. 2018; Pillepich et al. 2018a; Springel et al. 2018). The IllustrisTNG simulations build on the original Illustris project through a series of numerical and physical model improvements (Weinberger et al. 2017; Pillepich et al. 2018b) over the original Illustris model (Genel et al. 2014; Vogelsberger et al. 2014a,b; Sijacki et al. 2015). In this work, we use the TNG100 simulation that involves a box of side length  $\sim 100$  Mpc as the original Illustris simulation. The baryon mass resolution is  $1.4 \times 10^6 M_{\odot}$  with a fixed softening length for stars of 0.7 kpc at  $z = 0$  and an adaptive softening for gas cells with a minimum of 0.185 comoving kpc. Throughout the text, cold gas refers to

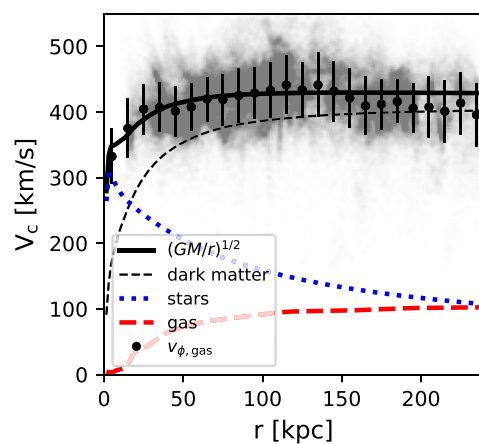


**Figure 2.** Circular velocity curve from the mass distribution as a function of radius. The tangential velocity of gas cells is overplotted with the grey scatter points. The extended gas disc at  $z = 0$  is rotating close to the circular velocity curve, and is therefore rotationally supported. Within the inner 20 kpc, the stellar mass dominates the mass budget.

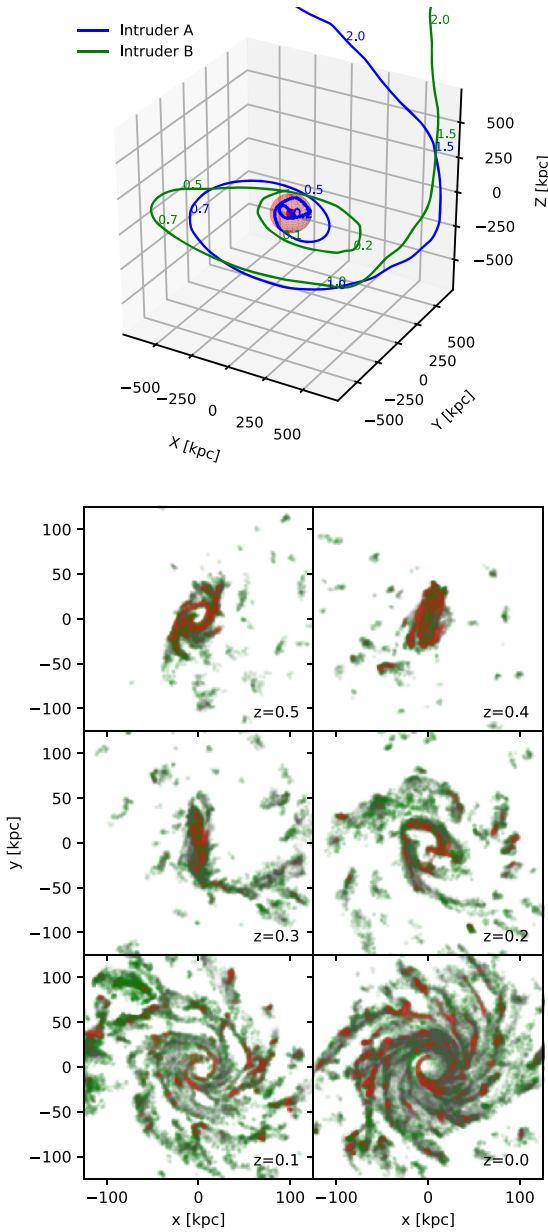
non-star forming gas with  $\log(T/K) < 4.2$  (to be compared with neutral hydrogen), while hot gas refers to gas with  $\log(T/K) > 6$ . Additionally, ‘star-forming gas’ is used when the gas density exceeds the threshold for star formation,  $n_{\text{sfr}} = 0.13 \text{ cm}^{-3}$ .

To identify GLSB galaxies, we use two-component (bulge+disc) surface photometry fitting (Xu et al. 2017) and create a candidate list. Through visual inspection, we identified one object (**Central**, hereafter), bearing a resemblance to Malin 1 in the stellar and gaseous morphologies. The SUBFIND ID of the Central at  $z = 0$  is 252245. Not only is the size of the disc in this galaxy the largest in the list, it has the largest cold gas mass in the entire galaxy catalogue.

Fig. 1 shows the stellar and gas discs from edge-on and face-on views. Without the stars formed later than  $z = 0.3$ , the Central is just a massive elliptical galaxy with a spherical stellar halo. The recently formed stars, on the other hand, are located in an extended disc with many apparent ‘stellar knots’. These knots are groups of newly formed stars from gas-rich clumps in the disc without associated dark matter haloes. Most of the stars in the disc are formed within the last 1.5 Gyr ( $z_{\text{form}} = 0.1$ , blue dots in Fig. 1). Also, there is not any clear stellar age gradient across the disc. Many of the features including the stellar ‘knots’, young stellar population, spiral structure, and lack of age gradient agree well with the observations of Malin 1 (Boissier et al. 2016).

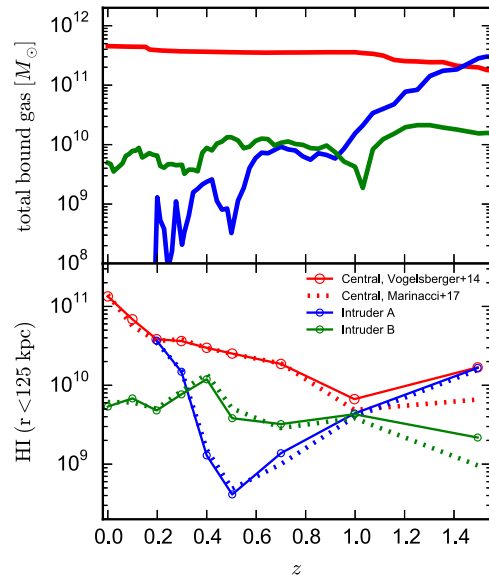
The gas distribution is in an extended and well-organized disc with a radius larger than 100 kpc. In the right-hand panels of Fig. 1, we show the cold gas in grey and star-forming gas in red. An exponential profile well describes the projected surface density profile of the gas disc, with a scale length of 37 kpc. Moreover, the surface density of the cold gas is one order of magnitude larger than the surface density of stars, highlighting the galaxy’s gas-rich nature.

Fig. 2 shows the circular velocity curves from the total mass distribution  $V_c = \sqrt{GM(r)/r}$  as well as the contribution from each component. The tangential velocity of the gas cells in the disc plane is shown with the grey scatter points. The gas disc rotates close to the circular velocity curve determined by the mass distribution. The gas rotation velocity stays flat up to 200 kpc, which qualitatively agrees with Lelli et al. (2010). Moreover, this galaxy has a  $V_{\text{max}} = 430 \text{ km s}^{-1}$  which is in excellent agreement with the values derived by Boissier et al. (2016).



**Figure 3.** *Top half:* Orbits of the galaxy pair, Intruder A and B, into the Central from  $z = 2$  to 0. The central red sphere has a radius of 125 kpc, the size of the final gas disc. We also label several redshifts along with galaxy trajectories to guide the readers. *Lower half:* The formation of a very extended gas disc from  $z = 0.3$  to  $z = 0$ . In addition to cold gas (grey) and star-forming gas (red), we show the gas cells with temperature between  $10^5$  and  $10^6$  K in green. Intruder A, with a peak  $V_{\max} = 350 \text{ km s}^{-1}$ , sank into the central potential faster than Intruder B, with a peak  $V_{\max} = 120 \text{ km s}^{-1}$ . While Intruder A is gas poor, there is much cold gas associated with Intruder B. The leading gas arm of Intruder B follows the trajectory of Intruder A, seen as the one arm structure at  $z = 0.3$ , and triggers efficient cooling of hot halo gas, which is confirmed with the location of gas with temperature between  $10^5$  and  $10^6$  K.

To shed light on the formation mechanism of such an extended stellar/gas disc, we use a merger tree (Rodríguez-Gomez et al. 2015) to trace back its formation history. Interestingly, we find the disc appeared only after  $z = 0.3$ , when a merger event occurred. The merger event involves a pair of in-falling galaxies with peak circular velocities of 350 and  $120 \text{ km s}^{-1}$  respectively. The top half of Fig. 3



**Figure 4.** *Top panel:* Total gravitationally bound gas mass as a function of redshift. While Intruder A has much gas until  $z = 1$ , it loses most of the gas since then. On the other hand, Intruder B has retained most of its gas mass until  $z = 0$ , despite having a lower  $V_{\max} = 120 \text{ km s}^{-1}$ . *Bottom panel:* The mass of neutral hydrogen within 125 kpc from the Central and the two intruders, respectively. For the Central, its neutral hydrogen mass has grown by a factor of at least three since  $z = 0.2$ . Among the Central and Intruder A or B, none of the three has gained this amount of neutral hydrogen prior to the merger event. The increase of neutral hydrogen within Intruder A since  $z = 0.5$  is caused by its proximity to the Central because the cold gas is not gravitationally bound to Intruder A.

shows the orbits of the two galaxies, which were orbiting around each other between  $z = 1.5$  and  $0.8$  while inspiralling into the Central. The more massive galaxy (**Intruder A**) sinks more rapidly in the potential well after  $z = 0.5$  due to stronger dynamical friction and completely merges with the Central at  $z = 0.16$ . Meanwhile, this intruder also completely disrupts the original gas disc of the Central (was visible as an edge-on disc in the centre of the gas image at  $z = 0.3$ ). Additionally, very little gas is directly delivered by Intruder A, which has lost most of its gas mass since  $z = 1$  when it was still fairly distant (625 comoving kpc) from the Central.

The less massive intruder (**Intruder B**), on the other hand, is quite gas-rich. The interaction between the galaxies in the pair has already liberated a great deal of gas from this object to form an elongated gas trail started from  $z = 0.4$ . Part of the leading arm of the cold gas closely follows Intruder A. By  $z = 0.3$ , the leading arm has already penetrated into 100 kpc from the Central. Since then an extended rotating gas disc, as shown in the lower half of Fig. 3, forms and builds up. By  $z = 0$ , Intruder B has not been completely disrupted yet. To see where the cold gas came from, we also colour the gas cells with temperature between  $10^5$  and  $10^6$  K in green. The location of gas at such a transitional stage closely follows the cold gas in the leading arm, which suggests that efficient cooling may have taken place at the interface between the cold gas and the hot halo, which we will show next.

All the three players in this cosmic dance are quite massive galaxies. In the top panel of Fig. 4, we show the total mass of gravitationally bound gas as a function of redshift. While Intruder A was gas-rich at high  $z$ , it has lost most of its gas mass since  $z = 1$ . On the other hand, Intruder B has retained most of its gas mass until  $z = 0$ , despite having a lower  $V_{\max}$ . We further compute the mass of

neutral hydrogen within 125 kpc from the three galaxies using two methods (Vogelsberger et al. 2014b; Marinacci et al. 2017a, their method 1). The results, shown in the lower panel with solid and dashed lines, respectively, demonstrate that the two methods are entirely consistent. The mass of neutral hydrogen within Intruder A has gradually declined, so has its total gas mass. The increase in the amount of neutral hydrogen within Intruder A is due to its proximity to the Central, but the cold gas is gravitationally bound only to the Central. The Central has grown its neutral hydrogen mass by a factor of at least three since  $z \sim 0.2$ .

At  $z = 0$ , the mass of cold gas within 125 kpc from the Central (the size of the final gas disc) is  $1.8 \times 10^{11} M_{\odot}$ , which is much higher than the total gas mass that can be delivered by Intruder A or B. The total mass of neutral hydrogen within the Central is similarly high,  $1.3 \times 10^{11} M_{\odot}$ . To identify the origin of the cold gas, we use tracer particles (Genel et al. 2013) to study their thermal histories. We select tracer particles within the cold gas disc and tracer particles in the hot halo gas, both within 125 kpc from the Central.

The left-hand panel of Fig. 5 shows the temperature histories of the cold gas in the Central identified at  $z = 0$ . In this plot, we show the gas temperature distribution evolution with redshift. The evolution of gas temperature shows that most of the cold gas mass came from the cooling of million-degree hot gas, which is triggered at  $z \sim 0.3$ . The central panel shows the distribution of cooling times for the hot gas within a radius of 250 kpc. Starting from  $z \sim 0.2$ , we observe a strong increase of the gas mass with a cooling time shorter than 1 Gyr. The right-hand panel shows the density fluctuations as a function of radius for hot gas, which is a necessary condition for efficient cooling. The largest fluctuations are observed to occur at  $z = 0.2$  and 0.1, when the cold gas mass sharply increased.

### 3 DISCUSSIONS

The fact that a similarly extended gas/stellar disc as Malin 1 has formed in a cosmological simulation is encouraging. As Boissier et al. (2016) argued, the distinct spiral structure and the lack of past bursts of star formation are difficult to explain by the ring galaxy model (Mapelli et al. 2008). A coplanar accretion of a dwarf can lead to an extended disc (Peñarrubia McConnachie & Babul 2006). However, this process cannot reproduce the observed flat gas rotation curve out to 100 kpc (Lelli et al. 2010) if Malin 1 has a similar mass as M31 (as in Peñarrubia et al. 2006). A slowly evolving disc with large angular momentum and a low level of star formation over cosmic time (Impey & Bothun 1989; Boissier et al. 2016) is also difficult to realize with our current cosmology and galaxy formation theory. Assuming our Galaxy has a typical spin, a spin parameter 20 times larger is exceptional ( $5\sigma$  away from the mean), although mergers can certainly help build up the spin parameter for massive halos (Zjupa & Springel 2017). More importantly, the disc has yet to survive frequent mergers or flybys since high  $z$  (Rodríguez-Gomez et al. 2017). Overall, it is challenging to reconcile a slowly evolving gas discs of  $\sim 100$  kpc size within a classical inside-out formation in  $\Lambda$ CDM (cold dark matter).

In contrast, the mechanism we identified in this study is able to explain the extended gas/stellar discs, the spiral structure, high gas fraction, as well as a flat rotation curve out to 200 kpc. The lack of an age gradient across the disc agrees with the recent observations by Boissier et al. (2016). The distribution of stellar ages in the extended disc (continuous star formation since  $z = 0.3$ ) is also consistent with the range (0.1 to 3 Gyr) found by Boissier et al. (2016). The exceptional cold gas mass can be explained by the cooling of hot halo gas triggered by an external supply of cold gas,

i.e. stimulated accretion. The entire picture has some similarities to the one proposed by Hagen et al. (2016). However, the galaxies in the pair are both more massive than typical dwarfs. In addition, a large mass fraction of the cold gas originated from the hot gas halo.

We find that only one galaxy contains a massive extended gas disc comparable to Malin 1 in the entire volume. Hot halo gas has been shown to be stable against cooling from tiny perturbations (Binney Nipoti & Fraternali 2009; Joung Bryan & Putman 2012). On the other hand, favourable conditions for hot halo gas to cool are present with an external supply of cold gas (Kereš & Hernquist 2009; Marinacci et al. 2011) or turbulence (Gaspari Temi & Brighenti 2017; Gaspari et al. 2018). In particular, the entropy mixing between cold gas and hot gas in the turbulent wakes is an effective channel for hot gas to cool and condense (Marinacci et al. 2011; Armillotta, Fraternali & Marinacci 2016). The cooling process in this study can also be viewed as a very special case in the top-down cold gas condensation framework, which plays a crucial role in active galactic nucleus feeding and star formation in early-type galaxies (for details, see Gaspari et al. 2017).

The large angular momentum of the final gas disc is a result of the orbital angular momentum in the cold gas stream. We note that the in-spiral of Intruder A has also spun up the hot gas substantially, from almost no rotation at  $z = 1$ , to a specific angular momentum within 250 kpc of  $1.5 \times 10^4 \text{ kpc km s}^{-1}$  at  $z = 0.3$ , which is  $\sim 50$  per cent of the value for cold gas. The angular momenta of cold and hot gas are also well aligned. It is possible that the rarity of Malin 1 analogues is a consequence of requiring a pair of galaxies on a specific in-spiral orbit with much cold gas in at least one member. Model refinements with higher resolution would be useful to determine the relative importance of each factor at play and reduce the numerical mixing.

Observationally, previous studies have hinted at a possible perturber close to Malin 1 (Moore & Parker 2006; Reshetnikov Moiseev & Sotnikova 2010). Our study suggests yet another potential culprit in building up the massive gas disc may still be hundreds of kpc away, which could be SDSSJ123708.91+142253.2 (Galaz et al. 2015). Some neutral hydrogen bridge between SDSSJ123708.91+142253.2 and Malin 1 will be a strong evidence for the scenario we discussed here. Also, the presence of an extended old stellar halo around Malin 1 can be revealed, in principle, with deep photometry to confirm it is a massive galaxy. Due to the large distance of Malin 1, these observational tests are non-trivial. Fortunately, there are similar nearby galaxies such as UGC 1382 (Hagen et al. 2016) which offer a more feasible alternative. Another important test is to establish whether the kinematics and metallicity pattern of the outer extended stellar/gas disc are distinct from the central regions, as expected from our scenario.

### 4 CONCLUSIONS

We have found a Malin 1 analogue in the 100 Mpc IllustrisTNG volume. This galaxy reproduces well the observed features of Malin 1's vast disc. The exceptional disc size is a result of hot gas cooling triggered by an ample supply of cold gas due to a pair of in-falling galaxies. This formation mechanism could reconcile the peculiarities of Malin 1's extended stellar disc within current galaxy formation theory in  $\Lambda$ CDM.

Finally, we note that the conditions that led to the formation of the simulated galaxy are similar to the present state of the Milky Way. Our Galaxy is interacting with a pair of galaxies, the Magellanic Clouds, and an extended gas structure, the Magellanic Stream. Theories suggest that the Clouds are on their first passage through

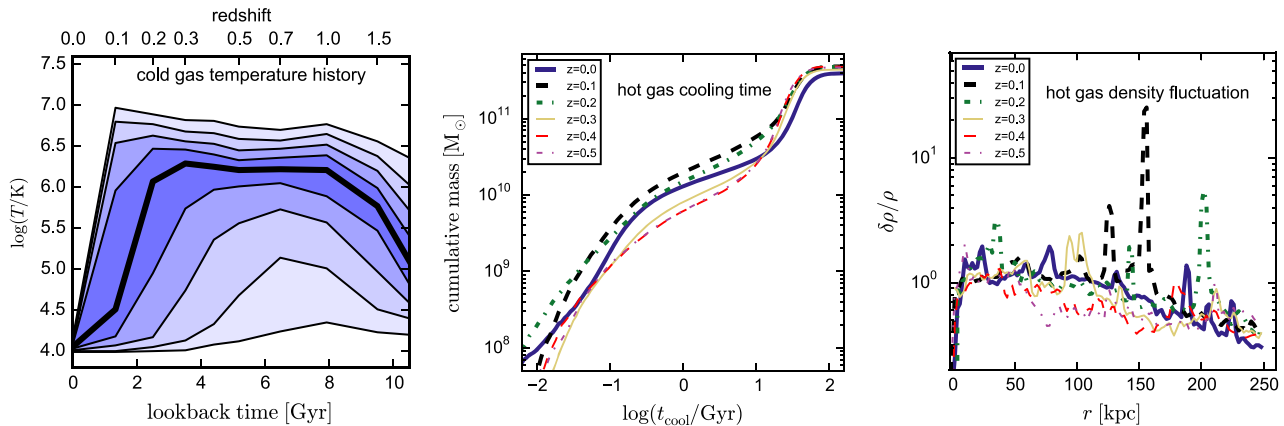


**Figure 5.** *Left-hand panel:* Gas temperature history of the cold gas identified at  $z = 0$  for the Central using tracer particles. We show the 10th, 20th up to 90th percentiles at each redshift. The median value of gas temperature (solid thick line) indicates more than half of the cold gas originated from million-degree hot gas at  $z = 0.3$ . *Middle panel:* The distribution of cooling times for the hot halo gas within 250 kpc from the Central at each redshift. We observe a strong increase of gas mass with cooling time-scale shorter than 1 Gyr between  $z \sim 0.2$  and 0. *Right-hand panel:* The density fluctuations  $\delta\rho/\rho$  of hot gas, a necessary condition for efficient gas cooling, as a function of radius at different epochs.

the Milky Way (Besla et al. 2007) and that the Stream resulted from the interaction between the Clouds (Besla et al. 2010). Based on these similarities to the object in IllustrisTNG, we speculate that the Milky Way may develop an extended disc of its own in the future through the stimulated accretion of gas from its hot halo.

## ACKNOWLEDGEMENTS

We thank Lea Hagen and Mark Seibert for stimulating discussions. YL acknowledges support from NSF grants AST-0965694, AST-1009867, AST-1412719, and MRI-1626251. MG is supported by NASA through Einstein Postdoctoral Fellowship Award Number PF5-160137 issued by the Chandra X-ray Observatory Center, which is operated by the SAO for and on behalf of NASA under contract NAS8-03060. Support for this work was also provided by Chandra grant GO7-18121X. VS, RP, and RW acknowledge support through the European Research Council under ERCStG grant EXAGAL-308037. VS, RP, RW, DX, and JZ would like to thank the Klaus Tschira Foundation at HITS. VS and JZ acknowledge support from the Deutsche Forschungsgemeinschaft through Transregio 33, ‘The Dark Universe’. The IllustrisTNG flagship simulations were run on the HazelHen Cray XC40 supercomputer at the High-Performance Computing Center Stuttgart (HLRS) as part of project GCS-ILLU of the Gauss Centre for Supercomputing (GCS). VS also acknowledges support through sub-project EXAMAG of the Priority Programme 1648 ‘Software for Exascale Computing’ of the German Science Foundation. MV acknowledges support through an MIT RSC award, the support of the Alfred P. Sloan Foundation, and support by NASA ATP grant NNX17AG29G. PT acknowledges support from NASA through Hubble Fellowship grant HST-HF2-51384.001-A awarded by the STScI, which is operated by the Association of Universities for Research in Astronomy, Inc., for NASA, under contract NAS5-26555. The Flatiron Institute is supported by the Simons Foundation.

## REFERENCES

Armillaotta L., Fraternali F., Marinacci F., 2016, *MNRAS*, 462, 4157  
 Barth A. J., 2007, *AJ*, 133, 1085  
 Besla G., Kallivayalil N., Hernquist L., Robertson B., Cox T. J., van der Marel R. P., Alcock C., 2007, *ApJ*, 668, 949

Besla G., Kallivayalil N., Hernquist L., van der Marel R. P., Cox T. J., Kereš, D., 2010, *ApJ*, 721, L97  
 Binney J., Nipoti C., Fraternali F., 2009, *MNRAS*, 397, 1804  
 Boissier S. et al., 2016, *A&A*, 593, A126  
 Bothun G. D., Impey C. D., Malin D. F., Mould J. R., 1987, *AJ*, 94, 23  
 Galaz G., Milovic C., Suc V., Busta L., Lizana G., Infante L., Royo S., 2015, *ApJ*, 815, L29  
 Gaspari M., Temi P., Brighenti F., 2017, *MNRAS*, 466, 677  
 Gaspari M. et al., 2018, *ApJ*, 854, 167  
 Genel S., Vogelsberger M., Nelson D., Sijacki D., Springel V., Hernquist L., 2013, *MNRAS*, 435, 1426  
 Genel S. et al., 2014, *MNRAS*, 445, 175  
 Hagen L. M. Z. et al., 2016, *ApJ*, 826, 210  
 Impey C., Bothun G., 1989, *ApJ*, 341, 89  
 Joung M. R., Bryan G. L., Putman M. E., 2012, *ApJ*, 745, 148  
 Kereš D., Hernquist L., 2009, *ApJ*, 700, L1  
 Lelli F., Fraternali F., Sancisi R., 2010, *A&A*, 516, A11  
 Mapelli M., Moore B., Ripamonti E., Mayer L., Colpi M., Giordano L., 2008, *MNRAS*, 383, 1223  
 Marinacci F., Fraternali F., Nipoti C., Binney J., Ciotti L., Londrillo P., 2011, *MNRAS*, 415, 1534  
 Marinacci F., Grand R. J. J., Pakmor R., Springel V., Gómez F. A., Frenk C. S., White S. D. M., 2017a, *MNRAS*, 466, 3859  
 Marinacci F. et al., 2017b, preprint (arXiv:1707.03396)  
 Moore L., Parker Q. A., 2006, *Publ. Astron. Soc. Aust.*, 23, 165  
 Naiman J. P. et al., 2018, *MNRAS*, 477, 1206  
 Nelson D. et al., 2018, *MNRAS*, 475, 624  
 Peñarrubia J., McConnachie A., Babul A., 2006, *ApJ*, 650, L33  
 Pillepich A. et al., 2018a, *MNRAS*, 475, 648  
 Pillepich A. et al., 2018b, *MNRAS*, 473, 4077  
 Reshetnikov V. P., Moiseev A. V., Sotnikova N. Y., 2010, *MNRAS*, 406, L90  
 Rodríguez-Gomez V. et al., 2015, *MNRAS*, 449, 49  
 Rodríguez-Gomez V. et al., 2017, *MNRAS*, 467, 3083  
 Sijacki D., Vogelsberger M., Genel S., Springel V., Torrey P., Snyder G. F., Nelson D., Hernquist L., 2015, *MNRAS*, 452, 575  
 Sprayberry D., Impey C. D., Bothun G. D., Irwin M. J., 1995, *AJ*, 109, 558  
 Springel V. et al., 2018, *MNRAS*, 475, 676  
 Vogelsberger M. et al., 2014a, *MNRAS*, 444, 1518  
 Vogelsberger M. et al., 2014b, *Nature*, 509, 177  
 Weinberger R. et al., 2017, *MNRAS*, 465, 3291  
 Xu D. et al., 2017, *MNRAS*, 469, 1824  
 Zjupa J., Springel V., 2017, *MNRAS*, 466, 1625

This paper has been typeset from a  $\text{\LaTeX}$  file prepared by the author.